A candidate dust disk surrounding the binary stellar system BD+31°643

Paul Kalas* **& David Jewitt**

Institute for Astronomy, University of Hawaii, 2680 Woodlawn Drive, Honolulu, Hawaii 96822, USA

Planetesimals are thought to form within the dense dust disks that surround young stars[1], although this process has not been observed directly. In contrast, the presence of dust disks around older, main-sequence stars can be used to infer that planetesimal formation has indeed occurred; dust is rapidly depleted in circumstellar environments, so a continuous supply of dust by the sublimation and collisional erosion of pre-existing planetesimals[2,3] is required to maintain a disk over the lifetime of the central star. The composition of the dust in such disks should provide clues regarding the composition of the planetesimals, and the structure of the disks (for example, gaps in the dust distribution) could be linked to physical interactions with unseen planets. To date, only one main-sequence star—β Pictoris—has been shown to have a dust disk that can be resolved optically[4]. Here we report the optical image of a candidate dust disk surrounding a main-sequence binary stellar system, BD+31°643. If the existence of this dust disk is confirmed by future observations, it would imply that binary stars may possess stable environments for planetesimal formation.

To establish criteria for identifying circumstellar nebulosities as candidates for near-edge-on disks, we use β Pic as a standard. The β Pic disk is a nearly linear, optical reflection nebulosity bisected by the star (Fig. 1), with a radius of at least 1,000 AU (60 arcsec)[5], but with significant asymmetries in the spatial distribution of dust[6,7]. Other explanations for the nebulosity, such as outflow phenomena, have been ruled out[8]. We therefore adopt the following criteria for finding disk candidates: (1) linear nebulosity bisected by the star, (2) morphological symmetry between the two sides of the nebulosity, (3) exclusion of outflow phenomena, and (4) exclusion of chance alignment with background objects.

As part of a current optical search for circumstellar disks[9], we obtained coronagraphic images of the B5V binary star BD+31°643. Located in the Perseus II star-forming region ~330 pc from the Sun, it illuminates the 2–3 arcmin scale reflection nebulosity IC348. IC348 was studied photographically as early as 1922[10], and more recently with a charge-coupled device (CCD)[11] and near-infrared array[12], but never with a stellar coronograph.

Observations were taken on 18 December 1995 UT at the University of Hawaii 2.2-m telescope on Mauna Kea. A coronagraph was used to artificially eclipse BD+31°643, as well as to suppress diffracted light within the telescope. We used broadband V and R Mould colour filters centred at 545 and 647 nm, respectively (approximating the Kron–Cousins colour system). Images were recorded with a 2,048 × 2,048 pixel CCD at a plate scale of 0.41 arcsec per pixel. Our image resolution was ~1.4 arcsec. In addition to BD+31°643, several stars devoid of circumstellar nebulosity were coronagraphically imaged under nearly identical conditions to sample the point-spread function (PSF).

The coronagraphic images of BD+31°643 reveal a nebulosity within 20 arcsec of the star that is linear, bisected by the star, and 1–2 mag arcsec^{-2} brighter than the arcminute-scale, diffuse nebulosity of IC348 (Figs 1, 2a). Subsequent, near-infrared images (taken without a coronagraph) resolve BD+31°643 into a previously known[13] binary. Isophotes of the nebulosity show an approximately symmetric, disk-like morphology (Figs 1, 2c), though the southeast extension appears longer and narrower than the northwest extension by ~15%. The midplane surface brightness gradient is approximately symmetric between the two extensions from 4 to 20 arcsec projected radius (Fig. 2b). The midplane gradient gradually flattens at smaller projected radii and can be characterized by two least-squares,

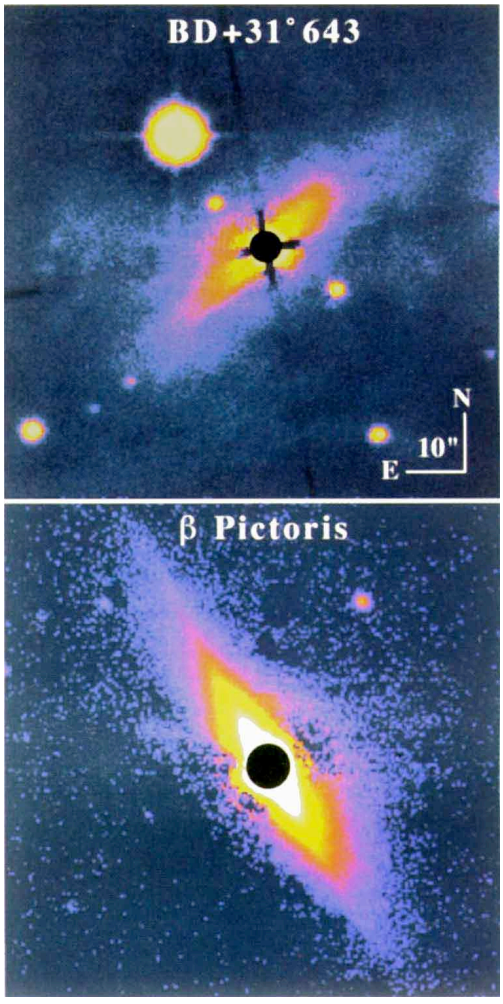

Figure 1 False-colour, R-band images of BD+31°643 (top) and β Pic (bottom; ref. 6) with effective integration times of 210 s and 890 s, respectively. A coronagraph was used to artificially eclipse BD+31°643 and β Pic with 3-arcsec and 6.5-arcsec diameter opaque spots, respectively (in these images, software-enlarged masks are shown, and the wires supporting the spots have been digitally removed). To study the disk near the edges of the spots, appropriately scaled and registered PSFs were subtracted from the central stars, as well as from the bright star (Gingrich 12) to the northeast of BD+31°643. For BD+31°643, an artificial PSF was created by fitting a seventh-order polynomial to the radial profile of a nearby, dust-free comparison star. We investigated possible subtraction errors due to the binarity of the BD+31°643 PSF and found them to be negligible beyond 4 arcsec radius. For Gingrich 12, its own light profile was sampled to the northeast (away from BD+31°643) to generate a similar artificial PSF for subtraction of scattered light. The net effect is a significant reduction of scattered light near BD+31°643 which allows the detection of the disk-like structure down to the edge of the occulting mask. The midplane of the BD+31°643 disk intersects the central binary at position angle PA = 131° ± 5°. Near-infrared data at K′ (λ = 2.2 μm) obtained by K. Jim (University of Hawaii) resolve the two stellar components. They have roughly equal magnitudes ($\Delta K' = 0.16 \pm 0.05$ mag), lie along a line with PA = 16.8° ± 2.0° and are separated by 0.60 ± 0.02 arcsec.

* Present address: Max-Planck Institute for Astronomy, Konigstuhl 17, D-69117 Heidelberg, Germany.

Table 1 Physical properties

	BD+31°643*	β Pic†
Spectral type	B5V	A5V
Stellar mass	$2 \times 5 M_{\odot}$	$1.5 M_{\odot}$
Apparent visual magnitude	+8.5	+3.8
Absolute visual magnitude	− 1.2	+2.7
Effective temperature	15,400 K	8,200 K
Luminosity	$2 \times 830 L_{\odot}$	$6 L_{\odot}$
Age	$\leq 10^7$ yr	$\geq 10^7$ yr
Distance	330 pc	16.4 pc
V surface brightness at 6″	20.0 mag arcsec^{-2}	16.3 mag arcsec^{-2}
Colour relative to star	Blue	Neutral
Midplane surface brightness	$r^{-0.3}$ (4″–7″), $r^{-1.9}$ (7″–20″)	$r^{-3.8}$–$r^{-4.1}$ (6″–16″)
Radial number density	$r^{+1.7}$ (4″–7″), $r^{-0.7}$ (7″–20″)	$r^{-2.8}$–$r^{-3.4}$ (6″–24″)
Observed radius	20″ (6,600 AU)	60″ (1,000 AU)
Length asymmetry	15%	20%
Inclination	0°–10°	0°–5°
Depleted region (radius)	2,300 AU	1–30 AU
Dust cross-section	8×10^{31} cm^2 (5″–20″)	7×10^{28} cm^2 (5″–40″)

In rows 2 and 6, we assume that the two components of BD+31°643 have approximately equal mass and luminosity. In rows 11,12 and 17, numbers in parentheses indicate the range of disk radii in arcsec where measurements were made and/or properties derived.
* Parameters obtained from refs 16, 28–30.
† Parameters obtained from refs 3, 6–22.

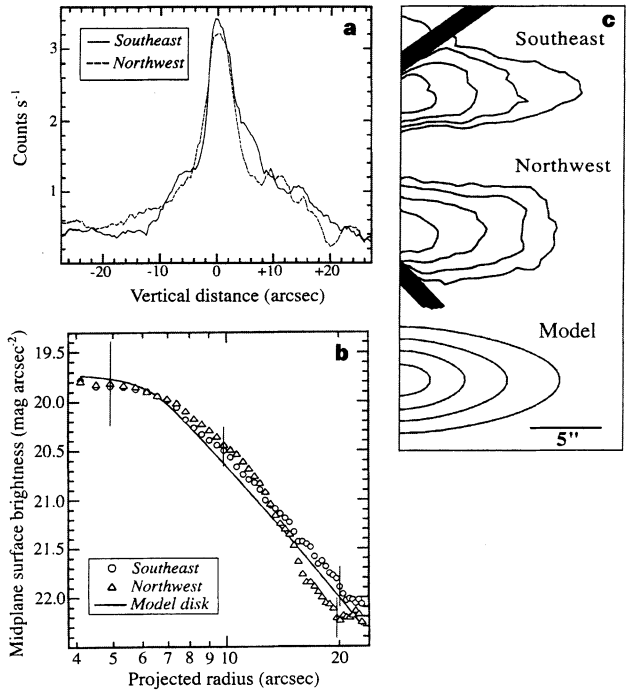

Figure 2 V-band data and model fits to the disk-like nebulosity around BD+31°643. **a**, Profiles perpendicular to the disk midplane at $r = 8$ arcsec (projected radius). The disk appears as a sharp feature ($|z| \leq 6$ arcsec, where z is the vertical distance from the disk midplane), superimposed on a broad bump ($6'' < |z| \leq 15''$) and the diffuse, arcminute-scale IC348 nebulosity ($|z| > 15''$). We define the outer radius of the disk, $r = 20$ arcsec, as the point where the disk can no longer be distinguished from the broad bump. **b**, Surface brightness along a strip 1.2-arcsec wide centred along the midplanes of each extension. To isolate disk light, the background nebulosity was sampled 6 arcsec north and south of the midplane (see **a**), the mean background was fitted with a third-order polynomial, which was then used to subtract light along the direction of disk midplane. The downturn in surface brightness within ~7 arcsec radius is seen in both extensions and in our R-band data (it is also evident before the subtraction of the background nebulosity). The scatter of points along the curves indicates the magnitude of statistical uncertainty (~0.1 mag arcsec^{-2}). However, the systematic uncertainty due to the background nebulosity is the dominant source of error, which we estimate and show as error bars at radii of 5, 10 and 20 arcsec. We also plot the midplane surface brightness of a model circumstellar disk which is depleted of material within 7 arcsec radius (see text). **c**, Surface brightness isophotes in V beginning from 5 arcsec projected radius (contour interval, 0.5 mag arcsec^{-2}; outer contour, 21.5 mag arcsec^{-2}). The data were rotated and transposed such that the star lies to the left, and the north side of each extension is up. Dark bars represent regions blocked by the occulting spot wires. The subtraction of background nebulosity introduces an uncertainty in the morphology of the outer contour of ~15%. The isotropic scattering model disk discussed in the text is shown for comparison.

power-law fits from projected radii 4 to 7 arcsec, and 7 to 20 arcsec (Table 1).

This morphology is inconsistent with collimated bipolar outflows (such outflows typically have an asymmetric appearance at visible wavelengths and occur during the pre-main-sequence phase of stellar evolution)[14,15], and there is no spectroscopic evidence for outflow in previous studies of this star[16]. That BD+31°643 has been established as the primary source of illumination for the larger-scale IC348 nebulosity, and that 12-μm and 60-μm emission from this region is centred on the binary[16], both indicate that the features nearest the binary are due to dust physically associated with BD+31°643 and not a chance alignment with a background object. The bright nebulosity meets our criteria for the optical detection of a near-edge-on circumstellar disk candidate.

We use a model of scattered light from dust arranged with the geometry of a disk[17] to fit the observed morphology and midplane surface brightness. Isophote shapes are fitted by model disks having inclinations $\leq 10°$ from edge-on (Fig. 2c). For example, an isotropically scattering model dust disk, inclined 10° away from edge-on, with an $r^{+1.7}$ increase in number density from 4 to 7 arcsec (r is radial distance), and an $r^{-0.7}$ decrease in number density from 7 to 20 arcsec fits our data (Fig. 2b, c). The radial number density gradient beyond 7 arcsec radius is flatter than derived for the β Pic disk ($\sim r^{-3}$; ref. 6), but comparable to our Solar System's zodiacal dust cloud (r^{-1}; ref. 18).

The model fits imply a centrally depleted region that is significantly larger in BD+31°643 than in β Pic (Table 1)[7]. Tidal interaction with the binary may create the central depletion of material near BD+31°643, as well as the asymmetries in disk structure[19]. The binarity of BD+31°643 has been recorded since 1881, but only a fraction of the orbit has been observed[13]. Further observations are required to clarify the orbital parameters, as well as to confirm the existence of the central depletion. However, we note that our model fits do not provide a unique explanation for the flattening of the midplane surface brightness gradient. Spatial variations in particle properties, such as the size distribution and composition, are not incorporated into the models, but may have a significant effect on the appearance of the nebulosity.

Table 1 compares the physical properties of the two stars and nebulosities. BD+31°643 is 20 times more distant than β Pic, 3.9 magnitudes (absolute) brighter, but is viewed through 2.8 magnitudes of visual extinction[20]. We measure $V - R = 0.2 \pm 0.2$ for both the disk and ambient nebulosity at 10 arcsec radius, whereas the star has $V - R = 0.5$ (refs 11, 21). The bluer colour of the nebulosity is consistent with previous findings[11] and indicates that the dominant particle size, a, is smaller than the wavelength of light, that is, $a \approx 0.1$ μm. However, the uncertainty of our measurements precludes an accurate assessment of possible colour gradients due to changes in particle size or composition.

We estimate from our optical data that the total dust scattering cross-section of BD+31°643 is three orders of magnitude larger than β Pic (Table 1). However, as BD+31°643 occupies a larger volume, the radial optical depths along the midplanes of both disks are $\tau \approx 10^{-3}$. If we assume dominant grain sizes of $a \approx 0.1$ μm for BD+31°643, and $a \approx 1$ μm for β Pic[22], then we infer from the total

scattering cross-sections approximate dust masses of 10^{-6} solar masses ($10^{-6}\,M_\odot$) for BD+31°643, and $10^{-8}\,M_\odot$ for β Pic (assuming a particle density $\rho = 1\,\mathrm{g\,cm^{-3}}$ and an albedo $A = 0.1$). These must be lower limits because we have not measured scattered light within 5 arcsec radius of either star, nor have we considered the likely presence of larger, unseen bodies.

In the absence of a significant gaseous component to the disk, forces such as Poynting–Robertson (PR) drag and radiation pressure will deplete the small dust surrounding BD+31°643 on short timescales. For a particle radius $a = 0.1\,\mu\mathrm{m}$, density $\rho = 1\,\mathrm{g\,cm^{-3}}$, distance from the star $r = 2,000$ AU and luminosity $L_* = 1,660\,L_\odot$ (where $L_\odot$ is the solar luminosity), the PR decay time is $t_{PR} = 0.2 \times 10^6$ yr. Even more significant is radiation pressure, which will blow out dust in an optically thin system if the ratio of radiation pressure to central gravity is $\beta > 1$. For a given particle size and composition, β scales very roughly as the ratio of stellar luminosity to stellar mass and is 40 times larger for BD+31°643 than for β Pic. Extrapolating from the β values calculated for various grain sizes and compositions around β Pic[23], we estimate that ~0.1-μm grains at 2,000 AU from BD+31°643 will be blown out to 6,000 AU on 10^3-yr timescales. The dominance of the radiation force over stellar gravity implies that the observed, disk-like structure is not centripetally supported and is therefore fundamentally different from the 10–100 AU-scale accretion disks detected around pre-main-sequence stars[24].

The age of BD+31°643 is probably greater than the 6×10^5 yr required for a BV5 star to reach the main sequence[25], but less than the $(5–7) \times 10^6$ yr age of the IC348 cluster[26]. The fact that the lifetime of 0.1-μm dust is orders of magnitude shorter than the age of the star argues that the dust within 6,000 AU is replenished. Erosion of larger bodies has been suggested as a source of replenishment for the β Pic disk[8]; adopting this suggestion, the inclination distribution of dust observed around BD+31°643 may reflect the inclination distribution of unseen parent objects. These parent bodies have either been partially cleared, or were prevented from forming near the stars due to tidal interactions, PR drag, collisions or other destructive forces. They are present at ~10^3 AU radii where they continue to replenish 0.1-μm-sized dust grains. If we assume an age of ~10^6 yr and a dust lifetime of ~10^3 yr, then the disk has been replenished 1,000 times over. Using the observed disk mass of ~$10^{-6}\,M_\odot$, we estimate that the mass of precursor objects is ~$10^{-3}\,M_\odot$ (a lower limit). The parental dust cloud (that is, the larger-scale IC348 nebulosity) still surrounds the disk and binary, and the entire system may represent an intermediate stage of evolution between embedded protostars (for example, the proto-binary system IRAS16293 − 2422[27]) and isolated, main-sequence stars such as β Pic.

Additional observations are required to test the disk interpretation of the nebulosity surrounding BD+31°643, to measure the gas content associated with the dust, and to clarify the relationship of the disk-like structure with the surrounding dust cloud. If its disk nature is confirmed, BD+31°643 represents an exceptional opportunity to examine the evolution and stability of planetesimals located around a binary stellar system. □

Received 20 May 1996; accepted 10 January 1997.

1. Weidenschilling, S. J. & Cuzzi, J. N. *Protostars and Planets III* (eds Levy E. H. & Lunine, J. I.) 1031–1060 (Univ. Arizona Press, Tucson, 1993).
2. Nakano, T. *Mon. Not. R. Astron. Soc.* **230,** 551–571 (1988).
3. Backman, D. E. & Paresce, F. in *Protostars and Planets III* (eds Levy, E. H. & Lunine, J. I.) 1253–1304 (Univ. Arizona Press, Tucson, 1993).
4. Smith, B. A. & Terrile, R. J. *Science* **226,** 1421–1424 (1984).
5. Smith, B. A. & Terrile, R. J. *Bull. Am. Astron. Soc.* **19,** 829 (1987).
6. Kalas, P. & Jewitt, D. *Astron. J.* **110,** 794–804 (1995).
7. Lagage, P. O. & Pantin, E. *Nature* **369,** 628–630 (1994).
8. Artymowicz, P. in *Proc. IAP Meeting on Circumstellar Dust Disks and Planet Formation* (eds Ferlet, R. & Vidal-Madjar, A.) 47–65 (Editions Frontieres, Paris, 1994).
9. Kalas, P. & Jewitt, D. *Bull. Am. Astron. Soc.* **25,** 1353 (1993).
10. Hubble, E. *Astrophys. J.* **56,** 400–438 (1922).
11. Witt, A. N. & Schild, R. E. *Astrophys. J. Suppl. Ser.* **62,** 839–852 (1986).
12. Zinnecker, H., McCaughrean, M. J. & Wilking, B. A. in *Protostars and Planets III* (eds Levy, E. H. & Lunine, J. I.) 429–495 (Univ. Arizona Press, Tucson, 1993).
13. Eggen, O. J. *Astron. J.* **68,** 483–514 (1963).
14. Edwards, S., Ray, T. & Mundt, R. in *Protostars and Planets III* (eds Levy, E. H. & Lunine, J. I.) 567–602 (Univ. Arizona Press, Tucson, 1993).
15. Staude, H. J. & Elsasser, H. *Astron. Astrophys. Rev.* **5,** 165–238 (1993).
16. Snow, T. P., Hanson, M. M., Seab, C. G. & Saken, J. M. *Astrophys. J.* **420,** 632–642 (1994).
17. Kalas, P. & Jewitt, D. *Astron. J.* **111,** 1347–1355 (1996).
18. Lamy, P. L. & Perrin, J.-M. *Astron. Astrophys.* **163,** 269–286 (1986).
19. Artymowicz, P. & Lubow, S. H. *Astrophys. J.* **421,** 651–667 (1994).
20. Strom, S. E., Strom, K. M. & Carrasco, L. *Publ. Astron. Soc. Pacif.* **86,** 798–805 (1974).
21. Fernie, J. D. *Publ. Astron. Soc. Pacif.* **95,** 782–785 (1983).
22. Paresce, F. & Burrows, C. *Astrophys. J.* **319,** L23–L25 (1987).
23. Artymowicz, P. *Astrophys. J.* **335,** L79–L82 (1988).
24. Basri, G. & Bertout, C. in *Protostars and Planets III* (eds Levy, E. H. & Lunine, J. I.) 543–566 (Univ. Arizona Press, Tucson, 1993).
25. Iben, I. *Astrophys. J.* **141,** 993–1014 (1965).
26. Lada, E. A. & Lada, C. J. *Astron. J.* **109,** 1682–1696 (1995).
27. Walker, C. K., Carlstrom, J. E. & Bieging, J. H. *Astrophys. J.* **402,** 655–666 (1993).
28. Underhill, A. & Doazon, V. *B Stars With and Without Emission Lines* (SP-456, NASA, Washington DC, 1982).
29. Schmidt-Kaler, Th. *Landolt-Bornstein, New Series, Group VI* (Springer, Berlin, 1982).
30. Racine, R. *Astron. J.* **73,** 233–245 (1968).

Acknowledgements. We thank G. Herbig and D. Backman for comments. The observations were made possible with the assistance of K. Jim, J. Gradie, B. Zuckerman and E. Becklin. P.K. was supported by the NASA Graduate Student Researchers Program; D.J. was funded by the NASA Origins of Solar Systems program.

Correspondence should be addressed to P.K.

High-energy ions produced in explosions of superheated atomic clusters

T. Ditmire, J. W. G. Tisch, E. Springate, M. B. Mason, N. Hay, R. A. Smith, J. Marangos & M. H. R. Hutchinson

Blackett Laboratory, Prince Consort Road, Imperial College of Science, Technology and Medicine, London SW7 2BZ, UK

Efficient conversion of electromagnetic energy to particle energy is of fundamental importance in many areas of physics. A promising avenue for producing matter with unprecedented energy densities is by heating atomic clusters, an intermediate form of matter between molecules and solids[1], with high-intensity, ultra-short light pulses[2–4]. Studies of noble-gas clusters heated with high-intensity ($>10^{16}\,\mathrm{W\,cm^{-2}}$) laser pulses indicate that a highly ionized, very high temperature micro-plasma is produced. The explosion of these superheated clusters ejects ions with substantial kinetic energy[3–5]. Here we report the direct measurement of the ion energy distributions resulting from these explosions. We find, in the case of laser-heated xenon clusters, that such explosions produce xenon ions with kinetic energies up to 1 MeV. This energy is four orders of magnitude higher than that achieved in the Coulomb explosion of small molecules[6], indicating a fundamental difference in the nature of intense laser–matter interactions between molecules and clusters. Moreover, it demonstrates that access to an extremely high temperature state of matter is now possible with small-scale lasers.

Such experiments have become possible owing to recently developed high peak power, femtosecond lasers which are based on chirped pulse amplification and are capable of producing focused light intensity up to 10^{14}–$10^{19}\,\mathrm{W\,cm^{-2}}$ (ref. 7). These high intensities have been used to study the production of highly charged ions from multi-photon ionization of individual atoms[8], and the optical ionization of small (2–10 atom) molecules, in which the resulting Coulomb explosion produces ions with kinetic energy of up to ~10–100 eV (ref. 9). At the same time, the production of hot (~1-keV), high-density plasmas by the intense irradiation of a solid has also been the subject of detailed studies[10]. Though the nature of the interaction of intense light with single atoms and bulk solid targets has been the subject of extensive investigation over the past decade,